ELSEVIER

International Journal of Mass Spectrometry 219 (2002) 559–575

International Journal of Mass Spectrometry

www.elsevier.com/locate/ijms

Stereochemical effects from doubly-charged iron clusters for the structural elucidation of diastereomeric monosaccharides using ESI/IT-MS

V. Carlesso, C. Afonso, F. Fournier, J.C. Tabet*

Laboratoire de Chimie Structurale Organique et Biologique, CNRS UMR 7613, Université Pierre et Marie Curie, 4 Place Jussieu, Bât F, 7éme étage, 75252 Paris Cedex 05, France

Received 5 February 2002; accepted 13 May 2002

Dedicated to Dr. Yannik Hoppilliard on the occasion of her 60th birthday.

Abstract

Several approaches may be used to contribute to the structural elucidation of carbohydrates. Distinction of diastereomeric monosaccharides is often a tedious task by mass spectrometry, and ultimately the monosaccharide stereochemistry must be determined. Diastereomers of glucose, mannose, galactose and talose stereochemically differ at the $C_{(2)}$ and $C_{(4)}$ positions and previous work described an efficient system used to differentiate these four monosaccharides easily. The approach was based on ESI mass spectrometry and scrutinized the behavior of a sugar molecule towards the iron(II) chloride and the resulting effects in the gas phase. The produced cationized monomeric $[MFe^{II}Cl]^+$ and dimeric $[M_2Fe^{II}Cl]^+$ ions as singly-charged species were studied by sequential MS/MS experiments. When submitted to low resonant excitation conditions these selected ions undergo fragmentation within a kinetic control (i.e., stereochemical effects on the rate constants of competitive unimolecular processes). Enhancement of stereochemical effects was displayed in the CID spectra of the cationized $[M_2Fe^{II}Cl]^+$ dimeric ions. The present work first reports the influence of the sample preparation on the produced cationized species using the electrospray process. Formation of doubly-charged cluster M_nFe^{2+} ions when the sugar molecule (M) is introduced in excess with the iron(II) chloride was observed. Secondly, behavior of these cluster ions under resonant excitation conditions reveals an increase of stereochemical effects compared with that observed in the case of singly-charged monomeric $[MFe^{II}Cl]^+$ and dimeric $[M_2Fe^{II}Cl]^+$ ions previously studied [Eur J Mass Spectrom 6 (2000) 421; Eur J Mass Spectrom 7 (2001) 331]. The dissociation pathways of doubly-charged complexes appeared to depend upon the *n* number of monosaccharides which constitute the formal ligand of the iron(II). M_nFe^{2+} cluster ions are useful to efficiently determine the stereochemistry of the investigated monosaccharides and represent an advantageous alternative for the structural elucidation of their respective stereochemistry. (Int J Mass Spectrom 219 (2002) 559–575)

Keywords: Monosaccharides; Iron(II); Stereochemical effects; Electrospray; Ion trap mass spectrometry; Cluster ions

1. Introduction

Carbohydrates have various biological functions and the studies of the action mechanisms present a growing interest. Many of their biological roles are relevant to cell-to-cell interactions (e.g., molecular recognition and communication) [3] as well as differentiation of cells and metastasis related to oligosaccharides linked to the surface of cell (e.g., microbial adhesion). Recent analytical approaches including separative techniques and spectroscopic methods are

* Corresponding author. E-mail: tabet@ccr.jussieu.fr

1387-3806/02/$ – see front matter © 2002 Published by Elsevier Science B.V.
PII S1387-3806(02)00742-X

suitable to elucidate complex molecular structures. Such a purpose needs determination of the monosaccharide composition and the oligosaccharide sequence with location of the sugar linkage and branching sites in conjunction with elucidation of the stereochemistry determination of the anomeric configuration and that of each glycosidic bond [4–6] either from intact carbohydrate systems or from hydrolyzed analytes [7,8]. Our interest concerns mainly the latter analytical approach. In this case, the first step is the identification of the molecular weight as well as the structure and stereochemistry of constitutive monosaccharides. Much research has been undertaken focused on the determination of the sugar molecular structure. Gas phase ionization as well as desorption/ionization techniques have been used for such a purpose. Positive ion chemical ionization (PICI) combined with tandem mass spectrometry (MS/MS) has shown stereochemical differences in the ion abundance from collision-induced dissociation (CID) spectra of both the MH^+ and adduct ions, as opposed to that of the unstable $M^{+\bullet}$ ions generated by electron impact which are generally absent from the EI mass spectra [9]. PICI experiments were carried out on carbohydrate derivatives to allow analysis by gas chromatography/mass spectrometry analysis [10,11]. Structural characterization has been carried out on underivatized carbohydrates especially for glycoconjugates in the negative ion mode (NICI) [12]. Desorption/ionization techniques such as fast atom bombardment (FAB) [13–15] and liquid-secondary ion mass spectrometry (L-SIMS) were extensively used to determine the oligosaccharide sequence and the branching information as well as its stereochemistry. Indeed, during the 1990s, several studies using such ionization mode have shown the potential of alkali and alkaline earth complexes to determine the oligosaccharide sequence and to obtain branching information as well as to locate the carbohydrate linkage [16]. Identification of glycosidic linkage stereochemistry and diastereomeric monosaccharide units were also accomplished [17].

More recently, matrix assisted laser desorption/ionization (MALDI) mass spectra have been used for efficient characterization of oligosaccharides [18–20]. The study of branched oligosaccharides show that the branching degree orients the produced fragment ions and the smallest alkali ion generated the greatest amount of fragment ions [20]. The use of PSD experiments like MS/MS were also useful as efficient characterization method of oligosaccharides [21]. Behavior of carbohydrates towards alkali ions has been extensively studied by Lebrilla and co-workers [22] from FT/ICR experiments. As application in MALDI-FT/ICR, the use of the “pelling” reaction for the alkali degradation of oligosaccharides allows a very efficient oligosaccharide sequencing [23]. Note that binding affinity of saccharides such as maltoheptaose has been investigated and presented a selectivity corresponding to the $H \ll Li < Na < K < Cs$ order under MALDI conditions [24]. Furthermore, the employment of an anion dopant demonstrates how negative ions in MALDI can be very useful for analysis of neutral oligosaccharides when the use of alkali coordinated complexes gives insufficient structural information [25]. However, they also showed that multiple metal coordination could be very structurally informative [26].

Alternatively, electrospray ionization (ESI) [27] presents complementary advantages to MALDI as it will be shown later. Under ESI conditions, generation in the gas phase of the intact desolvated quasi-molecular ions as well as the cluster ions of non-volatile and polar compounds from solution is considered as very useful for the investigation of the carbohydrate stereochemistry. Monosaccharides and oligosaccharides have been known for a long time to be particularly reactive toward alkali ions [28] and to generate stable quasi-molecular ions. More recently these effects have been seen with transition metallic ions [29]. In spite of the lack of extensive prompt fragmentations usually required for structural elucidation, these methods were successfully applied to the study of carbohydrates for distinguishing their respective stereochemistry by the use of MS/MS experiments.

Earlier, the group of Fura and Leary [30] studied the behavior of the Ca^{2+} and Mg^{2+} coordinated oligosaccharides toward collision-induced dissociations to locate the linkage position from linear and

branched oligosaccharides. They further investigated fragmentation patterns of metal–ligand complexes to provide information about the mono- and disaccharide stereochemistry [31]. This approach was successfully applied for larger size analytes constituted by a common triosyl core and using first row transition metal ions (i.e., Cu^{2+}, Mn^{2+}, Co^{2+} and Zn^{2+}) [32] as well as the Ca^{2+} and Sr^{2+} alkaline earth ion as ionizing agent [29,32]. Nevertheless, particular difficulties were found for preparing iron^{II}/carbohydrate complexes for such purposes although, the *N*-acetyl hexosamine analysis was developed using ferrocene boronate derivation [33]. These cationizing agents usually chosen for enhancing the detection of such molecules allow gas phase stabilization through charge retention at the metal cation. Their choice influences the reproducibility of the formation of very stable cationized molecules as well as a high desorption yield required for their efficient analysis using MS/MS methods. The fingerprint of ESI/MS is dependent upon the sample preparation and unfortunately, the relative abundances of the produced ions are not sufficiently reproducible, to be useful for distinguishing diastereomers without ambiguities. Actually, transition metal ions have been used because of their potential to favor covalent attachment in cationized molecules resulting in diagnostic fragment ions under various collision energy conditions [34]. The growing use of metal adduct ions in analytical tandem mass spectrometry results from reports on significantly increased structural information obtained for metal ion complexes with sugars, lipids and peptides. This trend differs to that observed from the chemistry of the protonated species which can provide less structural information. This is particularly due to the intrinsic reactivity of transition metal ions in the absence of a solvent and eventually, counter-ion effects.

A primary focus of research in our laboratory [1,2] has been to determine the stereochemistry of four monosaccharides cationized by Fe^{2+} generated from the $Fe^{II}Cl_2$ salt using electrospray combined with an ion trap mass spectrometer [3]. The experiments have been carried out on D -stereoisomers (i.e., glucose, mannose, galactose, and talose). The ultimate goal of this project is the development of a method for carbohydrate sequencing where metal–ligand systems are used to cationize the studied oligosaccharide in order to enhance structural differentiation using ESI/IT-MS/MS to be applied in future under HPLC coupling conditions with post-column introduction of metallic cation solution.

The model sugar was especially selected as a basis to develop a simple approach allowing the distinction of the axial/equatorial stereochemistry of hydroxyl groups located at the $C_{(2)}/C_{(4)}$ positions assuming mainly a $^4C_1$ chair conformation for the studied monosaccharide in aggregates (Scheme 1). Stable ion complexes prepared in solution were desorbed and dissociated into the ion trap cell using the resonant excitation mode. Activation of the produced cationized monomeric $MFe^{II}Cl^+$ and dimeric $M_2Fe^{II}Cl^+$ cluster ions depending upon the initial

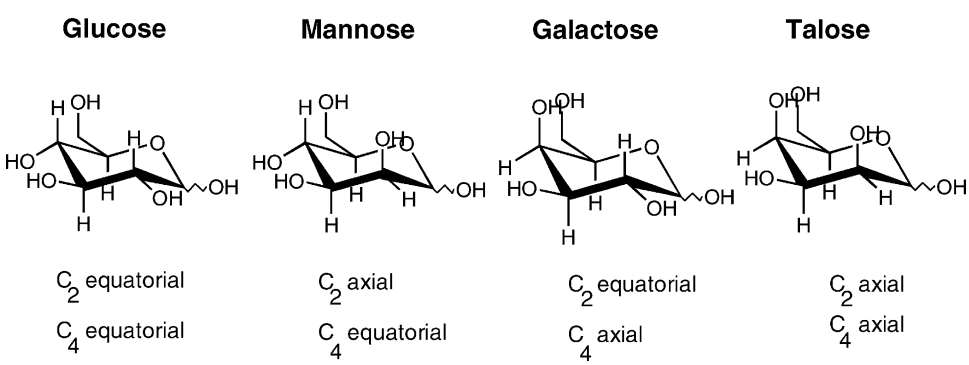

Scheme 1. Structures of the four monosaccharides examined in this study represented in their respective $^4C_1$ conformation.

conditions and allows an efficient method for the structural elucidation of monosaccharides to be establish. Stereochemical effects on ion fragmentations and ion abundances were made evident by energy resolved mass spectrometry (ERMS) breakdowns of the cationized monosaccharide complexes. The data demonstrated that diastereomers can be distinguished on the basis of reproducible ion abundances in CID spectra of the cationized species. Observed competitive fragmentations reflect the gas phase interactions between the sugar neutrals and the metallic ions and allow enhancement of stereochemical effects from CID experiments of the cationized dimeric ions.

The presented work reports the influence of sample preparation on the produced various cationized species under ESI conditions. The in situ production of doubly-charged multimeric M_nFe^{2+} aggregates was optimized using particular ESI conditions to reinforce stereochemical effects as observed using other transition metal cations [32] yielding $[M + Met^{II}]^{2+}$ (as well as $[M + Met^{II}Cl]^+$ and $[(M - H) + Met^{II}]^+$). The use of the cationized non-covalent multimers was based upon observation of the stereochimical and chiral distinctions of amino acids [35] as well as aliphatic diols [36] with the use of Cu^{2+} as reagent ion rather than Fe^{2+} which is more appropriate for saccharide analysis. From the latter, the CID processes of non-covalent cationized multimers have explored the role of the metal attachment site on the dissociation orientation according to the size of the revealed non-covalent M_nFe^{2+} species. In these species, iron(II) is bare in contrast with cationized monomeric $MFe^{II}Cl^+$ and dimeric $M_2Fe^{II}Cl^+$ clusters constituted by $Fe^{II}Cl^+$ a particular solvated species in which the chlorine anion is preserved. The resonant excitation of the M_nFe^{2+} ions represent an opportunity to show the effect of the naked iron(II) on the fragmentation pathway orientation. Another way of undertaking this study is to determine the possibility for the improvement of the stereochemical model of differentiation previously established by the resonant excitation of singly-charged cationized species [1,2].

2. Experimental

Mass spectra and sequential MS^n experiments were performed in ion trap mass spectrometer (ESQUIRE-Bruker, Bremen, Germany) equipped with an Analytica of Brandford (Brandford, CT, USA) external ESI source. Solutions containing monosaccharide and iron chloride salt ($FeCl_2$) in a 5:1 ratio (or 1:5 ratio) were prepared in a 1:1 mixture of acetonitrile/water. The solutions were diluted to achieve a final concentration of sugar of about 10^{-4} M which were introduced into the external electrospray source using a syringe pump included with the ESQUIRE system for direct sample infusion mode. Solution flowed at atmospheric pressure through a grounded stainless steel capillary. Heated N_2 at 200 °C was used as a drying gas to assist nebulization process. Ionization/desolvatation conditions were optimized for abundant cationized cluster ions M_nFe^{2+} (with the ^{56}Fe natural isotope major ions) that allowed reproducible sequential MS^n experiments to be performed. The *m*/*z* ratio range (noted in Thomson units [37]) used for the analytical scan was from 50 to 2000 Th. Resonant ion ejection occurred at $\beta_z = 2/3$ ($q_z = 0.78$) within a $\Delta(m/z)$ value of 0.4 Th (scan rate of 2000 Th/s). All ESI mass spectra were recorded in positive ion mode with a capillary voltage of 4 kV, end plate 3.5 kV, capillary exit voltage 100 or 40 V, skimmer voltage 10 V, hexapole rf 700 V_{p-p}, exit lens voltage −100 V and low *m*/*z* ratio injection cut-off (LMCO) values 40 and 80 Th.

Axial modulation (unknown amplitude) was also used in order to enhance the *m*/*z* resolution. Cluster $M_n{}^{56}Fe^{2+}$ ions were selected in the broadband isolation mode (4 Th as the isolation width) and submitted to resonant excitation for CID experiments with the helium buffer gas. ERMS experiments (energy resolved mass spectrometry) were performed particularly on the selected $M_3{}^{56}Fe^{2+}$ ions (*m*/*z* 298) using resonant excitation variation from 0.5 to 1.6 V_{p-p} by 0.1 V_{p-p} steps. Normalizing each experimental point as the ratio plotted ERMS breakdowns [(abundance of the considered fragment ion)/(∑ abundance of all ions recorded in the CID spectrum)].

Carbohydrates were purchased from Sigma–Aldrich (France).

3. Result and discussion

3.1. ESI mass spectra of glucose obtained using $FeCl_2$ as a cationizing reagent: effect of the relative concentration of sugar and iron(II) on the ionized cluster size and charge

Recorded ESI mass spectra of monosaccharides in the presence of the cationizing agent show mainly several cationized cluster ions with various natural isotopes of iron, ^{56}Fe (91.75%) being the most abundant which is accompanied by other natural isotopes such as ^{54}Fe (5.81%), ^{57}Fe (2.15%) and ^{58}Fe (0.29%). The chemical nature of these ions depends upon the relative concentration of the sugar and the iron(II) chloride salt as well as source conditions (i.e., the capillary exit and skimmer voltages) which influence the relative abundance distribution of the produced cluster ions.

3.1.1. Deficiency stoichiometry in sugar in favor of singly-charged aggregates (solutions containing monosaccharides and iron(II) chloride in a 1/5 ratio)

Under the present ESI conditions (i.e., capillary exit voltage 100 V, skimmer voltage 10 V and LMCO 40 Th), recorded ESI mass spectrum (Fig. 1) displays only singly-charged solvated ions corresponding to both the monomeric $M^{56}Fe^{II}Cl^+$ (*m*/*z* 271) and dimeric $M_2{}^{56}Fe^{II}Cl^+$ (*m*/*z* 451) cationized ions. As expected their relative intensities increase as the skimmer voltage decreases, and with the resulting decrease in their internal energy. Furthermore, by increasing the low mass cut-off of ion injection (without modification of the skimmer potential), the detection of cationized trimeric ions $M_3{}^{56}Fe^{II}Cl^+$ (*m*/*z* 631) can be enhanced. This results from a better ion storage at the higher q_z values (i.e., higher depth of the Dehmelt pseudo-potential well). However, a decrease in the stability of the non-covalent system is also expected during the injection step as the trapping q_z value rises due to the increase of the drive rf voltage. Indeed, energetical collisions during the injection

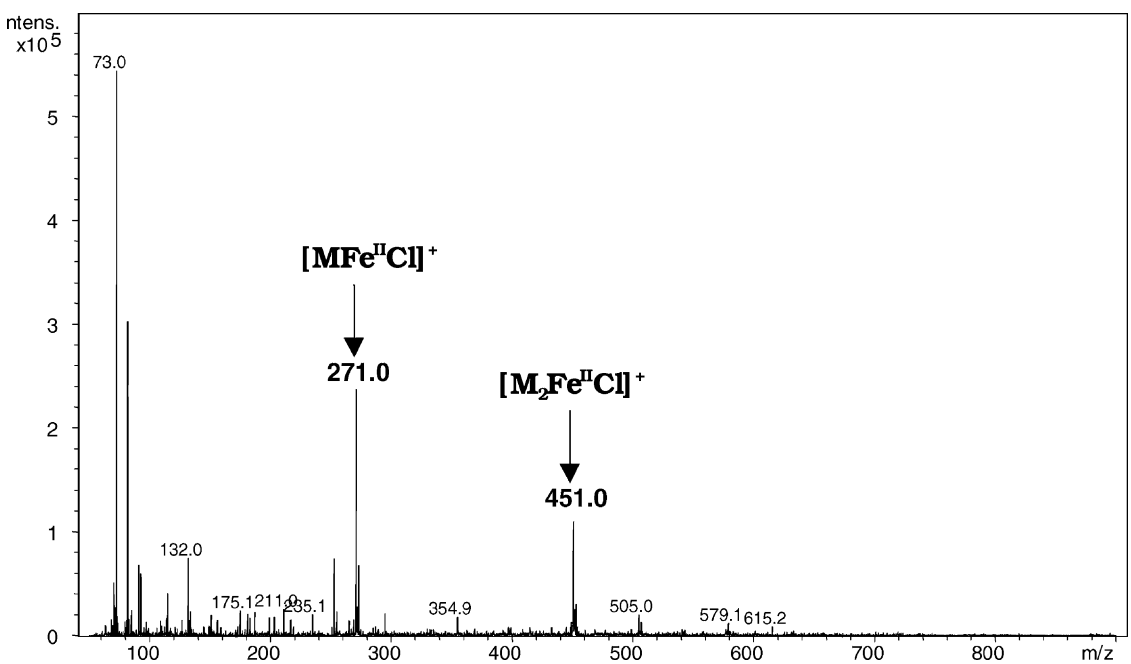

Fig. 1. ESI mass spectrum of glucose in presence of $FeCl_2$ solution in an 1/5 ratio and in a mixture 1:1 of acetonitrile water [1].

step are enhanced by the larger pseudo-potential well reached at higher injection q_z values. This effect was not observed in the present case, suggesting that these species are relatively stable towards CID processes.

3.1.2. Excess stoichiometry in favor of doubly-charged cluster ions (solutions containing monosaccharides and iron(II) chloride in a 5/1 ratio)

With the present conditions of sample preparation, doubly-charged cluster ions M_nFe^{2+} (with a n number of monosaccharides solvating directly or not the iron(II) center) are exclusively observed in ESI mass spectra. Furthermore, additional cluster ions with a lower abundance are detected at m/z 200, 290, 380, 470, 560, 650, 740, 830, 920, 1010, 1100 and 1190 (from $n = 2$ to 13) corresponding to the $[M_nHK]^{2+}$ ions. This behavior should reflect the selectivity of the cluster towards potassium rather than sodium, although the sodium adduct ions were generally observed as the main species for monosaccharide compounds desorbed from solution. One explanation can be offered by considering that the iron(II) cation significantly modifies the conformation of the solvating sugar, allowing a better shape of the host cavity in the sugar. The ion injection value of the LMCO modulates the observed relative abundance of the cluster ions, as shown in Fig. 2a and b. This emphasizes how the trapping parameters significantly influence the detected M_nFe^{2+} cluster ions in size and in abundance. The increase of the LMCO value enhances the storage efficiency of the larger M_nFe^{2+} cluster ions (from $n = 2$ to 13, Fig. 2b). A similar behavior was displayed for the heterocluster $[M_nHK]^{2+}$ ions which came with the M_nFe^{2+} iron sugar clusters.

Conversely, the decrease in the LMCO value induces a similar diminution of the n number of the ligand around the iron(II) in an ESI mass spectrum (from $n = 2$ to 5, Fig. 2a). This behavior can be explained by considering that the LMCO increase induces an enhancement of the ion internal energy of the injected ions as well as during the storage step related to the depth of the pseudo-potential well. Surprisingly, the larger the size of the M_nFe^{2+} ions the more abundant they become. This observation reflects the relative high stability of these non-covalent ions towards natural CID occurring in the trap cell. Singly-charged monomeric $[MFe^{II}Cl]^+$, dimeric $[M_2Fe^{II}Cl]^+$ and trimeric $[M_3Fe^{II}Cl]^+$ cluster ions are characterized under these experimental conditions by a similar trend as shown previously [1,2]. Note that a second distribution at higher m/z ratio (from $n = 6$ to 13) is weakly abundant (Fig. 2b) compared to the main distribution (from $n = 2$ to 5, Fig. 2a and b).

This trend can be explained by considering particular multimeric arrangement around the iron^{II} ion to yield one or two solvation sphere(s) constituted by several hexose units which give rise to formation of hexa-coordinated ion complexes. According to several theoretical studies, the interaction between the transition metal cation and the monosaccharide involves more than one hydroxylic groups (usually, 2 or 3 sites). This has been shown especially for Cu^{2+}, Mn^{2+}, Co^{2+} and Zn^{2+} as well as for Ca^{2+} for oligosaccharides such as the α 1–3, α 1–6 mannotriose and several analogs conserving a common triose core [32]. These oligosaccharides being covalent systems, the local metallic ion attachment at two or more OH sites on one of the hexose unit set is sufficient to generate stable complex ions. Alternatively in the present work, non-covalent cationized multimeric hexoses are formed instead to covalent adduct systems. It is very likely that solvation of iron^{II} must occur through several hexose units by one (and/or two) hydroxyl site(s) rather than by only one sugar (via more OH sites) of oligosaccharidic backbone. Consequently, the stabilization of iron^{II} multimeric systems ($n = 1$ to 4) may possibly result in the presence of zwitterionic-like forms for one (or several) monosaccharide(s) neighbored to Fe^{II} as shown in Scheme 2.

It is very likely that for deprotonation, the anomeric hydroxylic group must be mainly involved in this attachment. This assumption is based upon an investigation of the gas phase glucose properties as shown by Lebrilla and co-workers [38]. They demonstrated that the anomeric hydroxyl was the most acidic site although, AMI and ab initio calculations [39] indicate that the anomeric site is the most acid hydroxyl group for α-glucopyranone whilst the $C_{(4)}$ hydroxyl was the

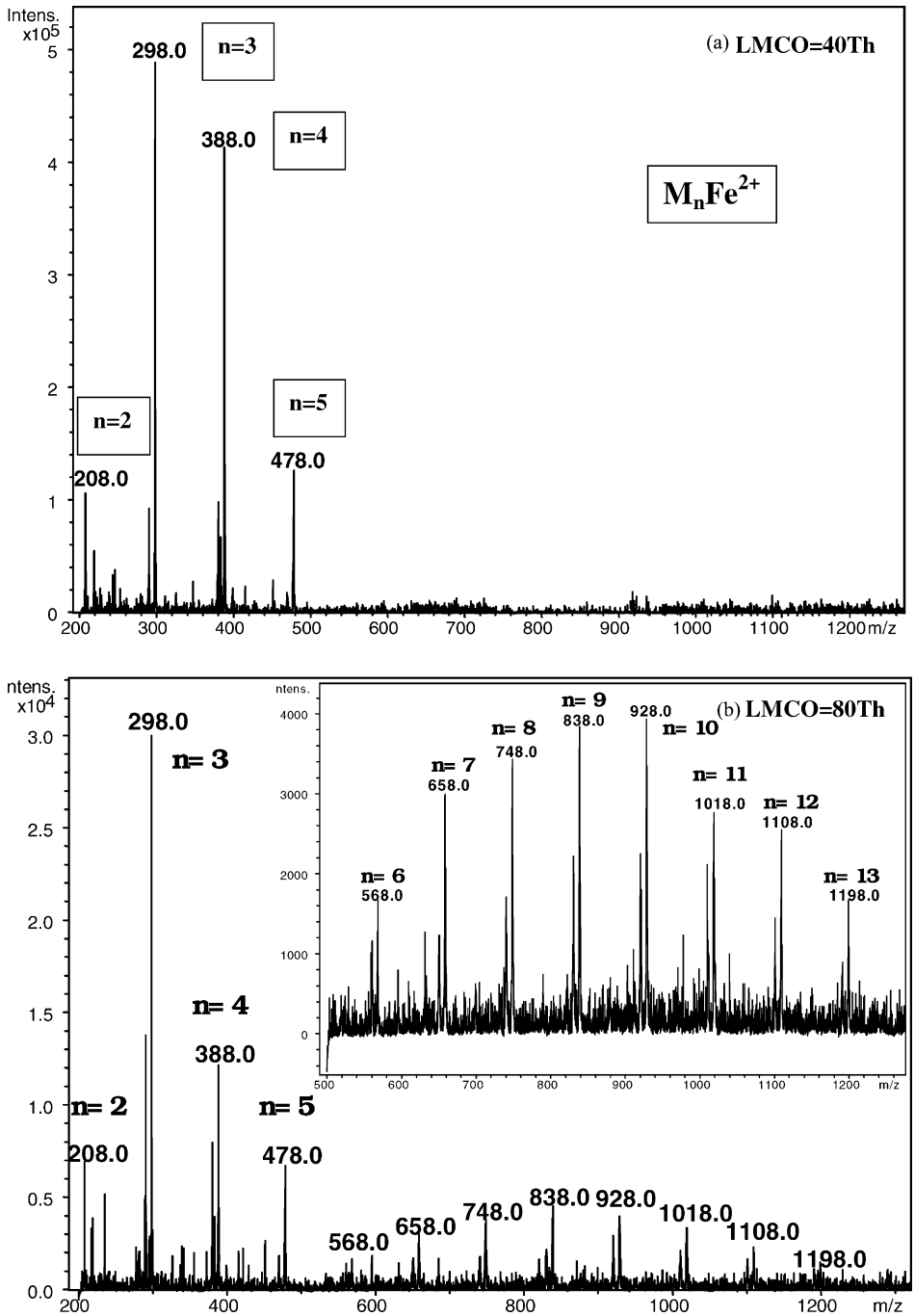

Fig. 2. ESI mass spectra (in same ESI conditions as described in Fig. 1) of solution containing glucose and iron(II) chloride in a 5/1 ratio, recording after ion injection according to low mass cut-off values of: (a) 40 Th and (b) 80 Th (in the window, a zoom of the higher *m*/*z* ratio ion distribution).

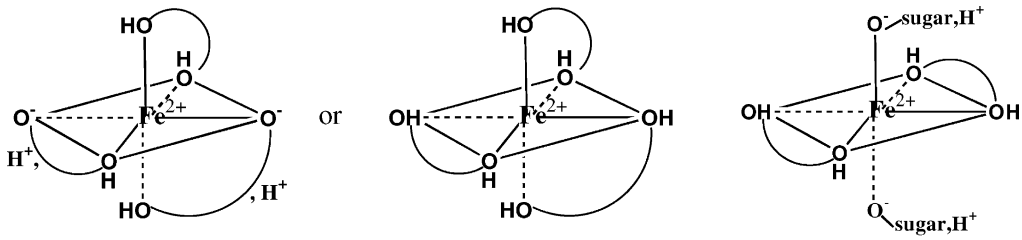

Form trimeric (a) Form trimeric (b) Form trimeric (c)

Scheme 2. Various isomeric hexa-coordonated iron^{II} trimers involving either (a) two zwitterionic hexose units and one uncharged unit or (b) only uncharged sugar forms and (c) iron^{II} tetrameric forms constituted by two singly-linked zwitterions and two doubly-linked uncharged monosaccharides.

most acid for the β anomer. Nevertheless, this behavior contrasts with the experimental observation from aqueous conditions. These authors considered fast alkoxid isomerization into various tautomeric species by internal proton transfer. Note that a partial metallic cation attachment at $C_{(6)}$ as well as at the ring oxygen ether (and linked oxygen atom of disaccharides) has been involved by Leary et al. [40]. The assumed presence of zwitterionic sugar forms has already been proposed and confirmed by calculation even if it was not the most stable form [41]. Thus, solvation of Fe^{2+} by 3 (or 4 as possible) zwitterionic hexose units according to a six-coordinated arrangement involving alkoxid/iron^{II} linkage(s) may result into a first stable solvation sugar layer around the doubly-charged iron^{II}. It may be expected that two or three hexoses (i.e., *m*/*z* 208 and 298, respectively) could be around the Fe^{2+} ion even though, the attachment of four or five sugar units (*m*/*z* 388 and 478, respectively) could be unstable because of a steric hindrance related to the size and conformation of each solvating sugar unit. In fact, for the M_5Fe^{2+} cluster ions, the fifth unit may solvate the external distant proton of the zwitterionic forms and it increase its stability. In a similar way, formation of an organized (or not) second layer of sugars can be considered by postulating the presence of several zwitterionic forms around Fe^{2+} which can be stabilized by an external multihexose layer.

Thus, the assumed existence of several solvation layers of monosaccharides around Fe^{II} considers: (i) a first layer neighbored to the doubly-charged cation solvated by alkoxid(s) of saccharide(s) with a zwitterionic form and (ii) a second layer distant to the iron^{II} core which solvates the protonated site(s) of the internal hexoses. The former allows observation of the $M_n{}^{56}Fe^{2+}$ series ($n = 2$ to 5) as *m*/*z* 208, 298, 388, and 478, and the latter yields *m*/*z* 568, 838, 928, 1018, 1108 and 1198 (from $n = 6$ to 13, respectively). The variation in abundances of both the series reflects a shielding effect of the doubly-charged iron(II) metallic centre which due to presence of the first layer constituted by more polarized hexoses (4 or 5). The created steric hindrance between aldopyranose reinforces this effect. Note that although, the strength characterizing the hydrogen bond interaction between hexoses (internal zwitterionic and external polarized units) is weak compared to that of internal salts (i.e., iron/alkoxid interaction), the hexose(s) of the second layer at periphery are sufficiently stable to be not released to yield more naked cluster ions during the cluster injection step by collision with the buffer and ambient gas. However, the second layer multimeric M_nFe^{2+} ions will decompose with higher rate constants than the first layer multimeric M_nFe^{2+} ions, which largely remain as shown in Fig. 2a and b.

3.1.3. Origin of clustering in the droplet

In order to rationalize the clustering processes which yield favorable observation of doubly-charged cluster ions at higher sugar concentrations (Fig. 2), we consider the story of cluster preformation in the

droplets. Examples of similar clustering under ESI conditions were previously described [42,43] in the case of arginine, histidine and leucine. Protonated amino acid clusters containing as many as 24 solute molecules and up to four charges were identified. The enlargement of the size distribution of these cluster ions increased also markedly by increasing the initial solute concentration. This clustering phenomenon provides insight into the chemistry of solute precipitation in solution and can be understood in terms of the ion evaporation model of Iribarne and Thomson [44,45].

The sequence of events taking place after the sample liquid leaves the injection needle is complex and has not been entirely elucidated yet. The liquid is dispersed into charged droplets from which solvent evaporates. In any droplets, the concentration of all but the most volatile solute species continues to increase until there remains only a cluster distribution of dry residue. These clusters retain whatever charges were on the droplet surface when evaporation stopped and consists of those solute molecules, which, during the evaporation of the solvent, were not released into the ambient gas as naked ions. It follows that at some time, in the evaporation process a droplet's liquid must become sufficiently saturated to start precipitation of a condensed solute phase, which favors in the final step of the cluster ions formation. These aggregate ions (more or less solvated) are finally transferred into the gas phase. For the examination and interpretation of these resulting cluster ions, it can be assumed that they desorb from the droplets more or less in accordance with the ion evaporation mechanism as proposed [44,45]. In the case of the low concentration solution, there is a clear competition between the Fe^{2+} cation and the solute molecules (as monosaccharide ligands). As a consequence, the produced ions are singly-charged and are solvated by carbohydrates and chlorine anion (i.e., $MFe^{II}Cl^{+}$ and $M_2Fe^{II}Cl^{+}$). The increase of the monosaccharide concentration induces a large quantity of solute species compared to the iron(II) cation. After the solvent evaporation, aggregation of monosaccharide neutrals in the droplets allows an efficient solvation of iron(II), and finally the M_nFe^{2+} cluster ions are liberated in the gas phase.

3.2. Distinction of diastereomeric sugars from CID experiments on cationized M_nFe^{2+} cluster ions

ESI mass spectra do not display fragment ions with large abundances because of the soft desolvation conditions at the skimmer. Since the structural elucidation of carbohydrates requires extensive fragmentation, sequential MS/MS experiments were performed using resonant excitation of the selected $[M_n{}^{56}Fe^{II}]^{2+}$ cluster ions. Under these experimental conditions, the recorded CID spectra exhibit product ions with highly reproducible abundances and present specific fragmentations from M_nFe^{2+} complexes characterized by a particular size. Indeed, clusters with 2 or 3 ligands yield CID spectra, which allow epimer distinction.

3.2.1. CID spectra of the larger size $M_n{}^{56}Fe^{2+}$ cluster ions (with $n \geq 4$): ineffective stereochemistry differentiation

Resonant excitation of doubly-charged $M_n{}^{56}Fe^{2+}$ ions ($n \geq 4$) yields a unique fragmentation pathway leading to a sugar unit loss to produce the $M_{n-1}{}^{56}Fe^{2+}$ clusters. This behavior occurs generally from non-covalent multimeric systems [46]. Stability toward collisions of $M_n{}^{56}Fe^{2+}$ with a higher polymerization degree decreases when voltage of the resonant excitation was increased. CID spectra of M_nFe^{2+} ($n \geq 4$) do not allow the stereochemistry of the four monosaccharides to be distinguished. This might suggest that the non-covalent associations in the second layer of the complex involved a lower influence of the steric hindrance effects than that which appeared from the first layer, directly linked to the Fe^{2+} cation. The absence of direct linkage with iron(II) is suggested by absence of covalent bond cleavage (e.g., a $C_2H_4O_2$ loss) of an hexose ring as occurs from singly-charged species [1,2].

3.2.2. CID spectra of the $M_n{}^{56}Fe^{2+}$ cluster ions with $n \leq 3$: stereochemical effects during covalent bond cleavage of the assumed first layer solvating iron(II)

In opposite to the larger size $M_n{}^{56}Fe^{2+}$ cluster ions (with $n \geq 4$), the $M_2{}^{56}Fe^{2+}$ and $M_3{}^{56}Fe^{2+}$ cluster

ions are characterized under CID conditions by extensive cleavage of covalent bond and non-covalent linkage, leading to singly- and doubly-charged product ions. This behavior supposes a high strength of direct interaction between the sugar of the first layer and the iron(II) metallic center.

CID spectra of the $M_3{}^{56}Fe^{2+}$ cluster ions (*m/z* 298) revealed three competitive dissociation pathways described by Eqs. (1)–(3) which correspond to:

(i) elimination of a sugar unit to yield the $M_2{}^{56}Fe^{2+}$ cluster ions (*m/z* 208), as expected for non-covalent systems (Eq. (1));
(ii) loss of water giving rise to formation of the doubly-charged $[M_3{}^{56}Fe^{II}–H_2O]^{2+}$ species (*m/z* 289) (Eq. (2));
(iii) complementary formation of cationized dimeric ions $[(2M - H) + {}^{56}Fe^{II}]^+$ (*m/z* 415) and protonated ions MH^+ (*m/z* 181) by charge separation (Eq. (3)).

Occurrence of the latter complementary ion pair supposes a bonding reorganization reaction around iron(II). This corresponds to Fe^{2+} attachment with an undetermined alkoxid group of one hexose (leading to cationized $[(2M - H) + {}^{56}Fe^{II}]^+$ dimers) and thus, the migration of the free proton to the hydroxyl group of the neighboring sugar ligand (leading to MH^+). This might take place by proton migration from the hydroxyl group activated by the iron(II) to a free OH group of a neighboring sugar unit yielding the $\{[(2M - H) + {}^{56}Fe^{II}]^+, MH^+\}$ intermediate able to dissociate into $[(2M - H) + {}^{56}Fe^{II}]^+$ (*m/z* 415), and MH^+ (*m/z* 181) by using the excitation energy to contend the coulomb barrier which appears as a transition state for charge separation.

$$\underset{m/z\,298}{M_3{}^{56}Fe^{2+}} \rightarrow \underset{m/z\,298}{M_2{}^{56}Fe^{2+}} \quad (1)$$

$$\underset{m/z\,298}{M_3{}^{56}Fe^{2+}} \rightarrow \left[\underset{m/z\,298}{M_3{}^{56}Fe^{II}–H_2O}\right]^{2+} \quad (2)$$

$$\underset{m/z\,298}{M_3{}^{56}Fe^{2+}} \rightarrow \left[\underset{m/z\,415}{(2M - H) + {}^{56}Fe^{II}}\right]^{+} + \underset{m/z\,181}{MH} \quad (3)$$

The other product ions displayed from CID spectra correspond to consecutive decompositions as described in Eqs. (4)–(7).

$$\underset{m/z\,208}{M_2{}^{56}Fe^{2+}} \rightarrow \left[\underset{m/z\,199}{M_2{}^{56}Fe^{II}–H_2O}\right]^{2+} \rightarrow \left[\underset{m/z\,190}{M_2{}^{56}Fe^{II}–2H_2O}\right]^{2+} \quad (4)$$

$$\left[\underset{m/z\,289}{M_3{}^{56}Fe^{II}–H_2O}\right]^{2+} \rightarrow \left[\underset{m/z\,280}{M_3{}^{56}Fe^{II}–2H_2O}\right]^{2+} \quad (5)$$

$$\left[\underset{m/z\,415}{(2M - H) + {}^{56}Fe^{II}}\right]^{+} \rightarrow \left[\underset{m/z\,355}{(2M - H) + {}^{56}Fe^{II}–C_2H_4O_2}\right]^{+} \quad (6)$$

$$\underset{m/z\,181}{MH^+} \rightarrow \left[\underset{m/z\,163}{MH–H_2O}\right]^{+} \rightarrow \left[\underset{m/z\,145}{MH–2H_2O}\right]^{+} \rightarrow \left[\underset{m/z\,127}{MH–3H_2O}\right]^{+} \quad (7)$$

3.2.3. Differentiation of the four monosaccharide isomers from the CID experiments performed on the $M_3{}^{56}Fe^{2+}$ cluster ions

Stereoisomer characterization from the cationized cluster $M_n{}^{56}Fe^{2+}$ ions with $n \geq 4$ is impossible because of the limited fragmentation induced by resonant excitation (i.e., unique loss of a sugar unit). On the other hand, the fingerprints provided from CID of the $M_3{}^{56}Fe^{2+}$ ions might be used to characterize the stereochemistry of isomeric monosaccharides under low and high resonant excitation amplitude (i.e., 0.8 and 1.5 $V_{p–p}$) and are presented in Fig. 3a and b.

The same major fragmentations of glucose and mannose are described by Eqs. (1) and (3), but they take place according to different relative abundances. Moreover, the $M_3{}^{56}Fe^{2+}$ ion of glucose presents a consecutive water loss from the doubly-charged

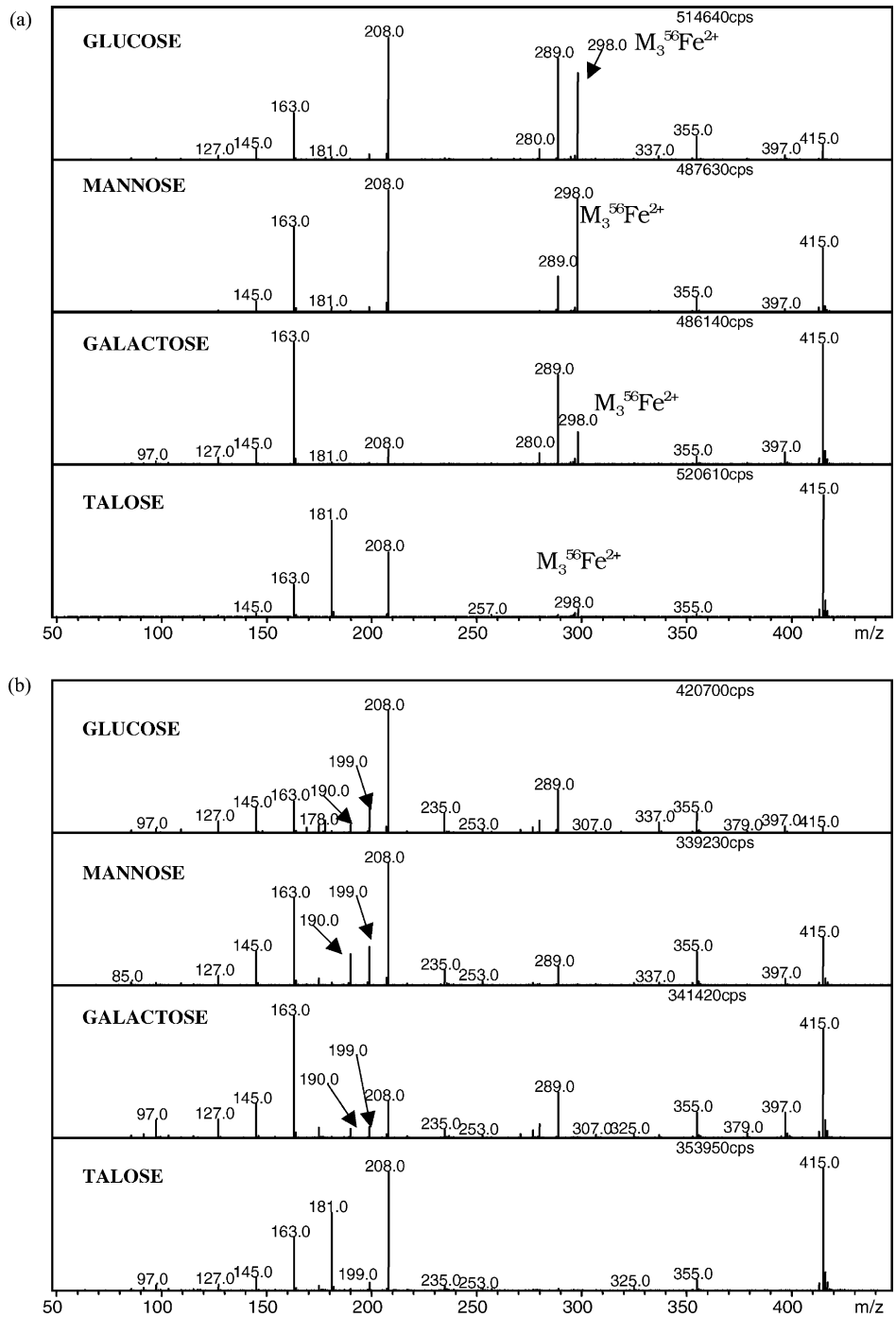

Fig. 3. CID spectra of the cationized $M_3{}^{56}Fe^{2+}$ cluster ions generated from each isomeric monosaccharide (glucose, mannose, galactose and talose) recorded at low and high resonant excitation amplitudes of: (a) $0.8\,V_{p-p}$ and (b) $1.5\,V_{p-p}$.

product ion *m/z* 289 to generate the doubly-charged second generation product ion *m/z* 280 (Eq. (5)), not observed from $M_3{}^{56}Fe^{2+}$ ions of the mannose. Alternatively, the main fragmentation pathways in case of galactose and talose are described by Eqs. (2) and (3). The latter process is mainly favored in the case of galactose under low amplitude conditions. Note that if the singly-charged *m/z* 415 ion is observed, it is not the case of the complementary *m/z* 181 ion, which appears very unstable and provides consecutive dissociations into *m/z* 163, 145, 127 and 97. Talose is the only one to generate an abundant MH^+ ion (*m/z* 181, i.e., Eq. (3)). The consecutive $3H_2O$ losses suggest that mainly the cyclic pyranoside structure is retained during these dissociations. Alternatively, the absence of a direct loss of 60 units from *m/z* 181 indicates that the acyclic structure plays a minor role. The rationalization of the stability (or not) of the protonated hexose, *m/z* 181, could be done by considering closed pyranoside forms. Consequently, it is very likely that the conformation of the protonated hexose generated by dissociation of doubly-charged cationized trimers must be a $^4C_1$ chair which is more stable by 40 kJ/mol for glucose and galactose [47] than the $B_{3,0}$ boat confirmation which predominates for mannose [48]. Talose studied here as well, is alone in presenting a significant stabilization for the *m/z* 181 protonated form (even under larger collision energy conditions) which means that it maintains its original conformation. It is likely that the trimer cluster may dissociate through hydrogen bond cleavage(s) rather than covalent C–C bond (or C–O ether bond) rupture. Finally, only for the ^4C chair confirmation, this may be preserved as form the previous acidic consideration.

It is likely that for talose, it may chelate the liberated proton resulting from the iron(II) attachment to another hydroxyl group. The other isomers (i.e., the glucose, mannose and galactose) do not present significantly the analogous MH^+ ions. The stereochemistry of these isomers does not permit such a chelation to stabilize the MH^+ ion. Consequently, the MH^+ product ions (*m/z* 163, 145, 127 and 97) are the only ions observed in CID spectra (Fig. 3a and b). In the case of talose; the other favored dissociation pathway is described by Eq. (1). Note also that doubly-charged cluster ions give essentially doubly-charged product ions by neutral loss, in spite of the presence of the coulomb potential barrier. This is particularly observed in the case of glucose, mannose and galactose. This trend reflects the existence of high barriers associated with formation of the complementary product ions MH^+ and $[(2M - H) + {}^{56}Fe^{II}]^+$ (Eq. (3)). These barriers are electrostatic due to charge repulsion between both the MH^+ and $[(2M - H) + {}^{56}Fe^{II}]^+$ partners and perhaps related to an eventual entropic effect due to the needed rearrangement yielding these diagnostic ions (Scheme 3). The level of these barriers, particularly the repulsive barrier is dependant upon the hexose stereochemistry as presented in Scheme 3. The level of these barriers can be qualitatively evaluated from the CID spectra (Fig. 3a and b) by considering the relative abundances of MH^+ (and its product ions) and $[(2M - H) + {}^{56}Fe^{II}]^+$ (and its product ions). The Coulomb barrier must be higher in the case of glucose as shown by the low abundances of the MH^+ and $[(2M - H) + {}^{56}Fe^{II}]^+$ ions and their respective product ions. This barrier decreases from glucose to mannose, from mannose to galactose and from galactose to talose. The entropic barrier related to the rearrangement reaction leading to formation of the product ions MH^+ and $[(2M - H) + {}^{56}Fe^{II}]^+$ cannot be estimated but should exist.

3.2.4. ERMS experiments from collision of the $M_3{}^{56}Fe^{2+}$ cluster ions (m/z 298)

The performed ERMS experiments improve stereoisomer differentiation. In this type of experiment the V_{p-p} amplitude of resonant excitation is increased stepwise by $0.1\,V_{p-p}$. The recorded breakdown curves for the four isomers are reported in Fig. 4. The data indicate that stereochemical differences in ion abundances are observed over the entire energy range investigated for the set of compounds. These ERMS breakdowns are reproducible in ion abundances (variation of ion abundances of ±5%) and in resonant excitation (variation of amplitude value used from 0.5 to $1.6\,V_{p-p}$) which reflects the particularity of ion trap mass spectrometry allowing through

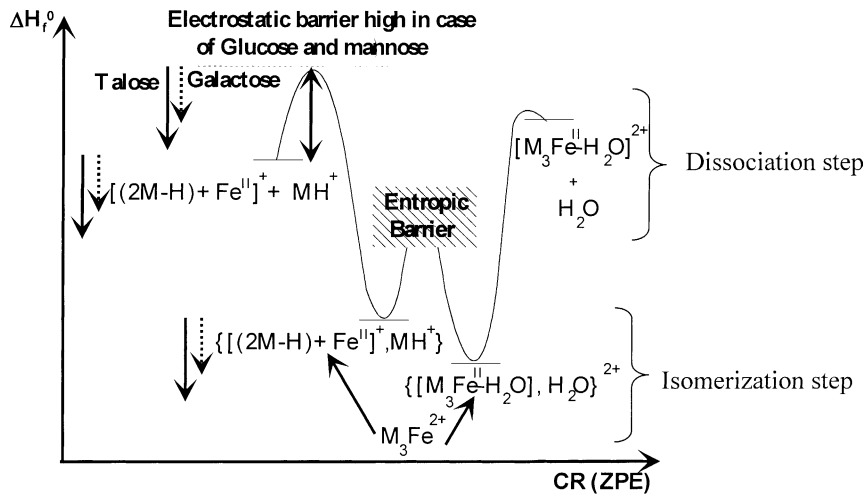

Scheme 3. Brauman potential pathway to interpret formation of the product MH^+ and $[(2M - H) + {}^{56}Fe^{II}]^+$ ions. Effect of the Coulomb repulsion related to the competitive dissociation of isomeric forms of cationized trimers.

the existence of the pseudo-potential well excitation energy accumulation [49].

The resonant excitation voltage effect on the competitive dissociations (Eqs. (1)–(3)) of the selected doubly-charged $M_3{}^{56}Fe^{2+}$ cluster ions (*m*/*z* 298) present breakdown specific for each diastereomeric hexoses. This differentiation is possible although up to approximately 1.1 V_{p-p}, the relative abundances of product ions are almost constant and the general trend of the ERMS breakdown is maintained (except for the consecutive losses of water molecules). From the breakdowns reported in Fig. 4 show several finding on the competitive processes:

(i) the desolvation such as the direct loss of one hexose unit (Eq. (1)) yielding $M_2{}^{56}Fe^{2+}$ (*m*/*z* 208) is favored for glucose and mannose and this, independently of the energy although it appears strongly for talose under high excitation energy conditions;

(ii) the product ions as *m*/*z* 415 and 181 (or *m*/*z* 163 due to fast consecutive loss of water) related to charge separation process (Eq. (3)) are enhanced as major pathway for talose and galactose. However, from the former hexose, the desolvation yielding *m*/*z* 208 (Eq. (1)) is increased up 1.3 V_{p-p} to become similar to the charge separation way. This behavior contrasts with galactose since at 1.6 V_{p-p}, it corresponds to less than 10% of total ionic current; and

(iii) the direct water loss (Eq. (2)) by covalent bond cleavage present a particular energy dependence. Below 0.8 V_{p-p} it competes with desolvation for glucose or with charge separation for galactose. Up to 0.9 V_{p-p}, its trend is to decrease strongly. For mannose, a similar behavior is observed but the *m*/*z* 208 abundance is relatively weak (or absent) for talose.

These observed trends are consistent with the proposed energy pathway of Scheme 3. Concerning the consecutive water losses, they are enhanced as energy raises from the singly-charged product ions such as MH^+ (or $[MH–H_2O]^+$ according to Eq. (7). Note that the exclusive loss of $C_2H_4O_2$ which occurs from the singly-charged $[(M - H) + {}^{56}Fe^{II}]^+$ ion (*m*/*z* 415, Eq. (6)) is slightly enhanced but it is maintained within a weak abundance. These breakdown dependences confirm that mainly the stereochemistry of the hexose units constituting the selected iron^{II} trimeric complexes preserved their initial structure as particularly shown by:

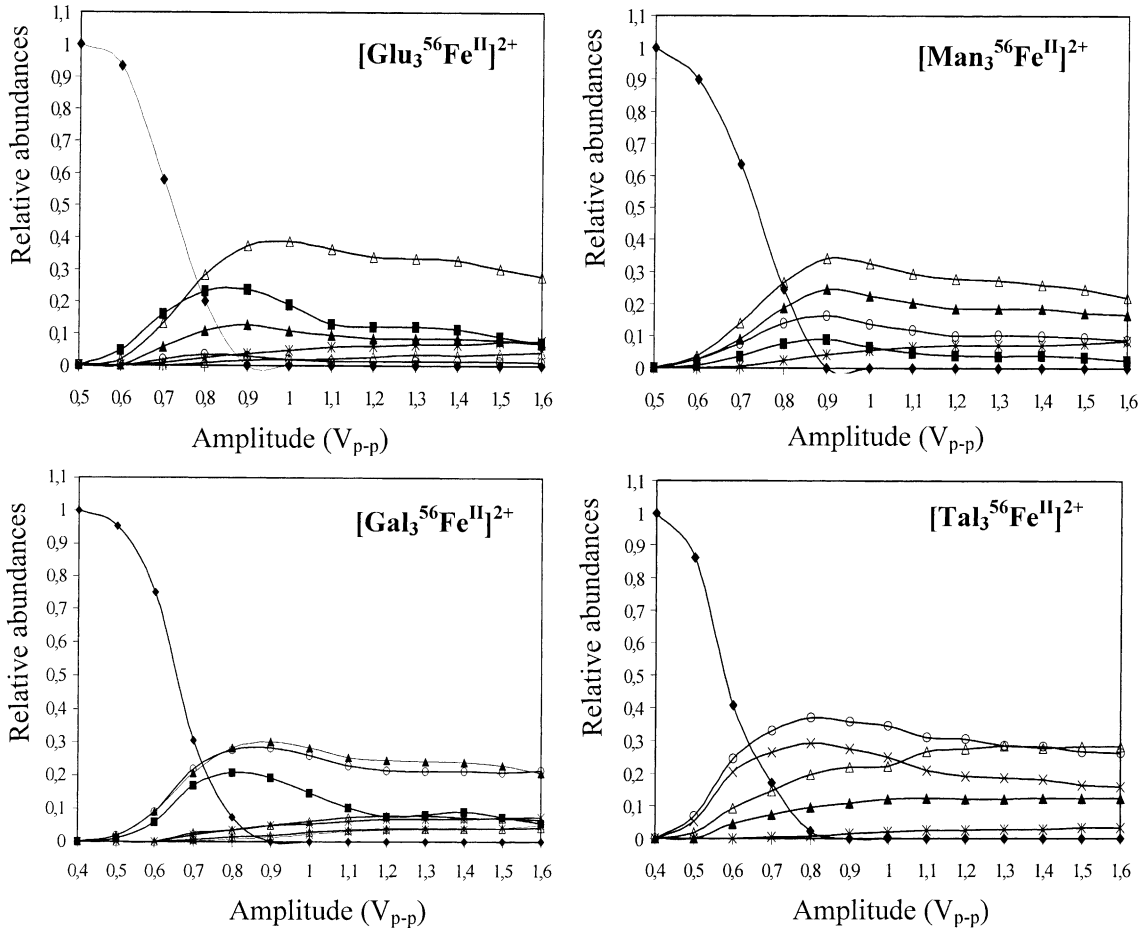

Fig. 4. ERMS breakdowns of each cationized $M_3{}^{56}Fe^{2+}$ cluster ions (*m*/*z* 298) prepared in ESI from: (a) glucose $[Glu_3{}^{56}Fe^{II}]^{2+}$, (b) mannose $[Man_3{}^{56}Fe^{II}]^{2+}$, (c) galactose $[Gal_3{}^{56}Fe^{II}]^{2+}$, and (d) talose $[Tal_3{}^{56}Fe^{II}]^{2+}$, recorded according to excitation amplitude rising from 0.5 to 1.6 V_{p-p} by step of 0.1 V_{p-p} (with ◆, ■, △, ×, ▲, ✳, ○ as the following ions: *m*/*z* 298, 289, 208, 181, 163, 145, and 415, respectively).

(i) the stereospecific presence of *m*/*z* 181 for talose, (ii) the variation of the extent loss of H_2O and $2H_2O$ from doubly-charged M_nFe^{2+} ions ($n = 2$ and 3) as well as

(ii) the competitive losses of H_2O and $C_2H_4O_2$ from the first generation product $[(2M - H) + {}^{56}Fe^{II}]^+$ ions independently of the resonant excitation conditions.

Consequently, ring opening isomerization may play only a minor role even at under higher energy excitation conditions.

3.2.5. Distinction of hexoses by CID of the $M_2{}^{56}Fe^{2+}$ cluster ions (m/z 208)

Furthermore, another alternative to distinguish the stereochemistry of the set of monosaccharides can be proposed considering resonant excitation of the $M_2{}^{56}Fe^{II}$ cluster ions (*m*/*z* 208). CID spectra presented (Fig. 5) for an voltage of 0.9 V_{p-p} display stereochemical effects but they are less important than those from $M_3{}^{56}Fe^{II}$ cluster ions (*m*/*z* 298) (Fig. 3). This results from decreased decomposition induced by resonant excitation of the $M_2{}^{56}Fe^{II}$ ions. The fragmentation pathways of the $M_2{}^{56}Fe^{II}$ lead to essentially

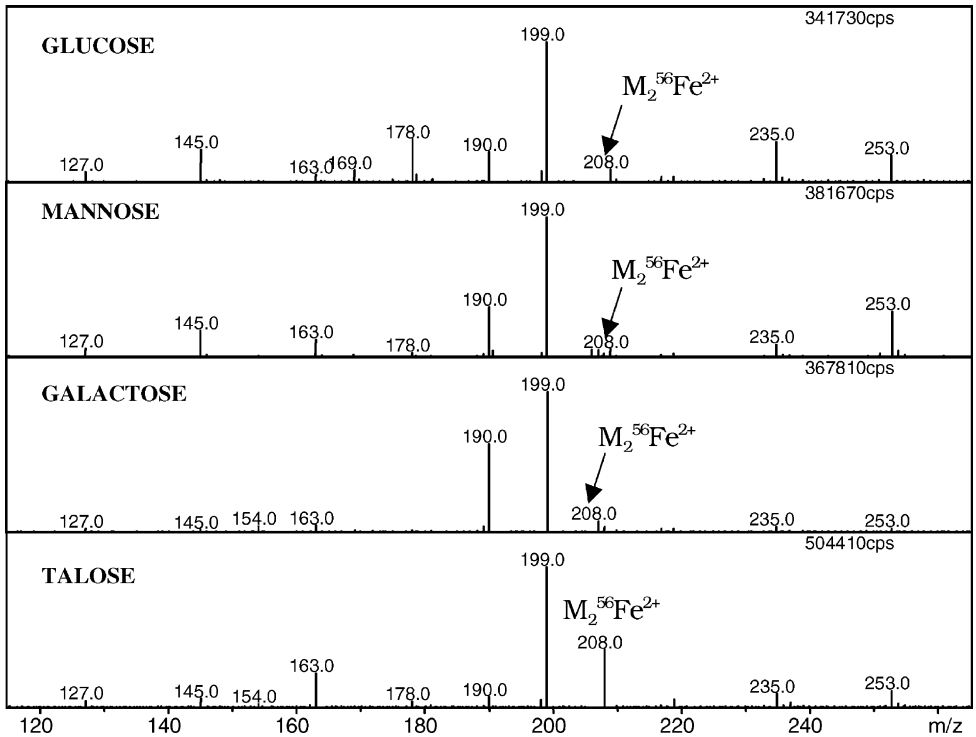

Fig. 5. CID spectra of the cationized $M_2{}^{56}Fe^{2+}$ cluster ions generated from each isomeric monosaccharide (glucose, mannose, galactose and talose), for a constant resonant excitation amplitude of $0.9\,V_{p-p}$.

doubly-charged fragment ions resulting from direct and consecutive water losses yielding the *m/z* 199 $[M_2{}^{56}Fe^{II}–H_2O]^{2+}$, and *m/z* 190 ($[M_2{}^{56}Fe^{II}–2H_2O]^{2+}$) product ions, and *m/z* 181 ($[M_2{}^{56}Fe^{II}–3H_2O]^{2+}$) for talose. The comparison of the relative abundances of these consecutive ions allows the monosaccharide stereochemistry to be distinguished. Especially as the glucose presents an abundant *m/z* 178 product ion resulting from $C_2H_4O_2$ neutral loss and was previously described in the study of the cationized monomeric singly-charged cluster of glucose [1].

By analogy with Eqs. (1)–(3) written to describe the observed fragmentation pathways of the $M_3{}^{56}Fe^{2+}$ cluster ions (*m/z* 298), the $M_2{}^{56}Fe^{2+}$ (*m/z* 208) dissociate by water losses according Eq. (2). The dissociation described by Eq. (1) (loss of a sugar unit) is not observed from the $M_2{}^{56}Fe^{2+}$ cluster ions. This can be rationalized by considering the required solvation sphere around the iron(II) cation, which is not shell-open if a sugar unit is lost. The fragmentation described by Eq. (3) is weakly favored in the case of the $M_2{}^{56}Fe^{2+}$ cluster ions. This results from the high electrostatic repulsion which prevents the formation of charge separation leading to the singly-charged MH^+ and $[(M-H)+{}^{56}Fe^{II}]^+$ product ions.

4. Conclusion

This work is a part of a larger study aiming to develop an approach to characterize carbohydrates using ESI combined with ion trap mass spectrometry after complexation with transition metals such as iron(II). Its primary objective was to distinguish the diastereomeric monosaccharides such as glucose, mannose, galactose and talose whose stereochemistry only differs at the hydroxyl sites at the $C_{(2)}$ and $C_{(4)}$ positions and should be extended to other monosaccharides with

stereochemistry change at other positions. The first part of this work [1] studied singly-charged cationized monomeric $[MFe^{II}Cl]^+$ and dimeric $[M_2Fe^{II}Cl]^+$ cluster ions. The second part was to modify the preparation conditions of sample containing monosaccharides and iron(II) chloride to generate various aggregates of monosaccharides such as the M_nFe^{2+} cluster ions, in view to enhance stereochemical effects which occur during resonant excitation conditions.

Two doubly-charged iron^{II} multimeric complexes M_nFe^{2+} are observed and are characterized by different n values, the major one with $2 < n \leq 4$ (and eventually 5) and the minor series which involves from $n = 6$ to 13. The stability of the main series of cluster ions is explained by assuming that Fe^{2+} is hexa-coordinated to three, four (or five) hexose units where several are isomerized into zwitterionic forms. This enhances stabilization strength of Fe^{2+} by the anomeric alkoxid sites. Under such structural arrangement, this first solvating layer presents one (or two) protonated hydroxylic group(s) (distant to the charged anomeric site), which can be solvated by an external second layer of several hexoses. The resulting steric hindrance effect of non-covalent hexose units as well as the less strength hydrogen bonds, explain why this external layer is less stable than the internal one and present a particular Gaussian distribution.

CID spectra of $M_n{}^{56}Fe^{2+}$ (with $n \geq 4$) do not allow the four monosaccharides to be characterized because they undergo only one unspecific cleavage (loss of a sugar unit). This behavior generally occurs for non-covalent multimeric systems, which often involve hydrogen bonding as well as cation solvation. Stereochemical effects were observed by CID experiments performed on $M_n{}^{56}Fe^{2+}$ (with $n = 2$ and 3). Under these experimental conditions, CID spectra obtained exhibit reproducible product ions within high abundances. They are specific for each monosaccharide stereochemistry. The best differentiation of epimeric structures was reached from resonant excitation of the M_3Fe^{2+} cluster ions. In this case, the sugar complexes decompose by similar pathways involving competitive and consecutive dissociations according to various rate constants, controlled by the $C_{(2)}/C_{(4)}$ stereochemistry. Therefore, monosaccharides can be distinguished without ambiguities in their CID spectra because they display significant variations in abundances of the product and second generation product ions. This approach can be advantageous in comparison with other methods described in the literature that require a chemical modification in solution. Benefit of this interesting in situ cationization is its adaptability in LC/MS experiments by direct post-column introduction. Finally, these approaches will be used in the future to characterize more complex systems such as disaccharides and oligosaccharides through the generation of: (i) singly-charged cluster ions such as cationized monomeric $[MFe^{II}Cl]^+$ ions (and dimeric $[M_2Fe^{II}Cl]^+$ forms) and (ii) doubly-charged M_3Fe^{2+} cluster ions which should improve the oligosaccharide sequencing as well as the carbohydrate linkage location and stereochemistry.

References

[1] V. Carlesso, F. Fournier, J.C. Tabet, Eur. J. Mass Spectrom. 6 (2000) 421.
[2] V. Carlesso, F. Fournier, C. Afonso, J.C. Tabet, Eur. J. Mass Spectrom. 7 (2001) 331.
[3] L. Stryer, Biochemistry, Freeman, New York, 1988, p. 331.
[4] D. Garozzo, G. Impallomeni, G. Montaudo, E. Spina, Rapid Commun. Mass Spectrom. 6 (1992) 550.
[5] V. Reinhold, B.B. Reinhold, C.E. Costello, Anal. Chem. 67 (1995) 1772.
[6] S.P. Gaucher, J.A. Leary, J. Am. Soc. Mass Spectrom. 10 (1999) 269.
[7] C.J. Biermann, Adv. Carbohydr. Chem. Biochem. 46 (1988) 251.
[8] M.F. Chaplin, J.F. Kennedy (Eds.), Carbohydrate Analysis, Oxford, New York, 1994.
[9] T. Radford, D.C. DeJongh, Carbohydrates, in: G.R. Waller (Ed.), Biochemical Applications of Mass Spectrometry, Interscience, New York, 1972 (Chapter 12).
[10] B. Fournet, G. Strecker, Y. Leroy, J. Montreuil, Anal. Biochem. 116 (1981) 489.
[11] O.S. Chizhov, N.K. Kochetkov, Meth. Carbohydr. Chem. 6 (1972) 540.
[12] F. Fournier, L. Ma, J.C. Tabet, C. Salles, Spectr. Int. J. 8 (1990) 273.
[13] J.W. Dallinga, W. Heerma, Biomed. Environ. Mass Spectrom. 18 (1989) 363.
[14] J.M. Berjeaud, F. Couderc, J.-C. Promé, Org. Mass Spectrom. 28 (1993) 455.
[15] B. Mulroney, J.C. Traeger, J. Mass Spectrom. 30 (1995) 1277.

[16] (a) Z. Zhou, S. Ogden, J.A. Leary, J. Org. Chem. 55 (1990) 5444;
(b) G.E. Hofmeister, Z. Zhou, J.A. Leary, J. Am. Chem. Soc. 113 (1991) 5964;
(c) J.A. Carroll, L. Ngoko, S.M. McCullough, E. Gard, A. Jones, C.B. Lebrilla, Anal. Chem. 63 (1991) 2526;
(d) Z. Staempfli, Z. Zhou, J.A. Leary, J. Org. Chem. 57 (1992) 3590;
(e) A. Fura, J.A. Leary, Anal. Chem. 62 (1993) 2805;
(f) J. Lemoine, D. Despeyroux, K.R. Jenning, R. Rosenberg, E. de Hoffman, J. Am. Soc. Mass Spectrom. 4 (1993) 197;
(g) J. Carroll, C.B. Lebrilla, L. Ngoko, C.G. Beggs, Anal. Chem. 65 (1993) 1582;
(h) L. Ngoka, J.F. Gal, C.B. Lebrilla, Anal. Chem. 66 (1994) 692;
(i) A.R. Dongre, V.R. Wysocki, Org. Mass Spectrom. 29 (1994) 700;
(j) V.N. Reinhold, S.-Y. Chan, S. Chan, B.B. Reinhold, Rapid Commun. Mass Spectrom. 11 (1997) 1353;
(k) S. Kurono, Y. Ohashi, T. Okananga, M. Hoshi, H. Hashimoto, Y. Nagai, J. Mass Spectrom. 33 (1998) 35;
(l) D.T. Li, G.R. Her, J. Mass Spectrom. 33 (1998) 644;
(m) S. Zapfe, D. Müller, Rapid Commun. Mass Spectrom. 12 (1998) 545.
[17] (a) G. Puzo, J.-J. Fournié, J.-C. Promé, Anal. Chem. 57 (1985) 892;
(b) J.M. Berjeaud, F. Couderc, J.-C. Promé, Org. Mass Spectrom. 28 (1993) 455;
(c) B. Multoney, J.C. Traeger, B.A. Stone, J. Mass Spectrom. 30 (1995) 1277;
(d) G. Smith, J.A. Leary, J. Am. Soc. Mass Spectrom. 7 (1996) 953.
[18] (a) B. Stahl, M. Steup, M. Karas, F. Hillenkamp, Anal. Chem. 63 (1991) 1463;
(b) B. Stahl, S. Thurl, J. Zeng, M. Karas, F. Hillenkamp, M. Steup, G. Sawatzki, Anal. Biochem. 223 (1994) 218.
[19] (a) K.K. Mock, M. Davey, J.S. Cottrell, Biochem. Biophys. Res. Commun. 177 (1991) 644;
(b) D.J. Harvey, P.M. Rudd, R.H. Bateman, R.S. Bordoli, K. Howes, J.B. Hoyes, R.G. Vickers, Org. Mass Spectrom. 29 (1994) 753;
(c) H. Perreault, C.E. Costello, J. Mass Spectrom. 34 (1999) 184.
[20] (a) D.J. Harvey, Rapid Commun. Mass Spectrom. 7 (1993) 614;
(b) A.K. Powell, D.J. Harvey, Rapid Commun. Mass Spectrom. 10 (1996) 1027.
[21] (a) B. Spengler, D. Kirsch, R. Kaufmann, J. Lemoine, Org. Mass Spectrom. 29 (1994) 782;
(b) J. Lemoine, F. Chirat, B. Domon, J. Mass Spectrom. 31 (1996) 908;
(c) D.J. Harvey, J. Chromatogr. A 720 (1996) 429;
(d) V. Havlicek, C. Kieburg, P. Novak, K. Bezouska, J.K. Lindhorst, J. Mass Spectrom. 33 (1998) 591.
[22] (a) S.T. Fannin, J. Wu, T. Molinski, C.B. Lebrilla, Anal. Chem. 67 (1995) 3788;
(b) J.A. Caroll, S.G. Penn, S.T. Fannin, J. Wu, M.T. Cancilla, M.K. Green, C.B. Lebrilla, Anal. Chem. 68 (1996) 1798;
(c) M.T. Cancilla, S.G. Penn, J.A. Carroll, C.B. Lebrilla, J. Am. Chem. Soc. 118 (1996) 6736;
(d) K. Tsenk, L.L. Lindsay, S.G. Penn, J.L. Hendrick, C.B. Lebrilla, Anal. Biochem. 250 (1997) 18.
[23] M.T. Cancilla, S.G. Penn, C.B. Lebrilla, Anal. Chem. 70 (1998) 663.
[24] M.O. Mohr, K.O. Bornsen, H.M. Widmer, Rapid Commun. Mass Spectrom. 9 (1995) 809.
[25] A.W. Wong, M.T. Cancilla, L.R. Voss, C.B. Lebrilla, Anal. Chem. 71 (1999) 205.
[26] S.G. Penn, M.T. Cancilla, C.B. Lebrilla, Int. J. Mass Spectrom. 195/196 (2000) 259.
[27] M. Yamashita, J.B. Fenn, J. Phys. Chem. 88 (1984) 4451.
[28] (a) B.B. Reinhold, S.-Y. Chan, S. Chan, V.N. Reinhold, Org. Mass Spectrom. 29 (1995) 736;
(b) M.R. Asam, G.L. Glish, J. Am. Soc. Mass Spectrom. 8 (1997) 987.
[29] M. Kohler, J.A. Leary, Int. J. Mass Spectrom. Ion Proc. 162 (1997) 17.
[30] A. Fura, J.A. Leary, Anal. Chem. 65 (1993) 2805.
[31] G. Smith, J.A. Leary, J. Am. Soc. Chem. 118 (1996) 3293.
[32] E.M. Sible, S.P. Brimmer, J.A. Leary, J. Am. Soc. Mass Spectrom. 8 (1997) 32.
[33] M.K. Young, N. Dinh, D.H. Williams, Rapid Commun. Mass Spectrom. 14 (2000) 1462.
[34] K. Linsley, S. Chan, B.B. Reinhold, V.N. Reinhold, S.-Y. Chan, Anal. Biochem. 219 (1994) 207.
[35] D. Zhang, W.A. Tao, R.G. Cooks, Int. J. Mass Spectrom. 204 (2001) 159.
[36] V. Carlesso, F. Fournier, J.C. Tabet, in: Proceedings of the 49th ASMS Conference on Mass Spectrometry and Allied Topics, Chicago, 2001.
[37] R.G. Cooks, L.A. Rockwood, Rapid Commun. Mass Spectrom. 5 (1991) 98.
[38] J.A. Caroll, D. Willard, C.B. Lebrilla, Anal. Chim. Acta 307 (1995) 431.
[39] B. Mulroney, J.B. Peel, J.C. Treager, J. Mass Spectrom. 34 (1999) 544.
[40] J.A. Leary, T.D. Williams, G. Bott, Rapid Commun. Mass Spectrom. 3 (1989) 192.
[41] Y.Y. Zheng, A. Staempfli, J.A. Leary, J. Am. Soc. Mass Spectrom. 4 (1993) 4943.
[42] C.K. Meng, J.B. Fenn, Org. Mass Spectrom. 26 (1991) 542.
[43] N.V. Krasnov, Y.S. Kusner, O.A. Mirgorodskaya, V.I. Nikolaev, G.G. Nikolaeva, Sov. Phys. Tech. Phys. 33 (1988) 1283.
[44] J.V. Iribarne, B.A. Thomson, J. Chem. Phys. 64 (1976) 2287.
[45] B.A. Thomson, J.V. Iribarne, J. Chem. Phys. 71 (1979) 4451.
[46] M. Peschke, A.T. Blades, P. Kebarle, J. Am. Chem. Soc. 122 (2000) 10440.
[47] M.K. Dowd, A.D. French, P.J. Redly, Carbohydr. Res. 264 (1994) 1.
[48] M.D. Leavell, S.P. Gaucher, J.A. Leary, J.A. Taraszka, D.E. Clemmer, J. Am. Soc. Mass Spectrom. 13 (2002) 284.
[49] M. Krahmer, K. Fox, Int. J. Mass Spectrom. 190/191 (1999) 321.